SLAC – PUB – 3827
November 1985
T/E

Extended Technicolor Signatures at the SSC

PETER ARNOLD*

Institute for Theoretical Physics and Department of Physics

Stanford University, Stanford, California, 94305

and

CHRISTOPHER WENDT†

Stanford Linear Accelerator Center

Stanford University, Stanford, California, 94305

Submitted to *Physical Review D*

⋆ Work supported in part by the National Science Foundation, contract NSF – PHY – 83 – 10654, and the Department of Energy, contract DE – AC03 – 76SF00515.

† Work supported by the Department of Energy, contract DE – AC03 – 76SF00515.

ABSTRACT

We consider signatures at SSC of Extended Technicolor models that contain only one doublet of techniquarks. In these models, the ETC gauge bosons carry color and can be produced in the gluon-gluon subprocess of pp collisions. We find that the predominant signal is the production and decay of bound states of ETC gauge bosons. The bound state levels are split by the hyperfine interaction and the color force. A major decay mode yields $t\bar{t}Z^0$ in the final state. The bound states are expected to be narrow enough that one could observe their spectroscopy in this channel. For $\sqrt{s} = 40$ TeV, the cross section times branching ratio should be about 4 nb if the ETC boson mass is 1 TeV. The signal falls rapidly for larger masses due to the smaller effective gluon-gluon luminosity.

1. Introduction

In this paper, we investigate a signature of Extended Technicolor (ETC) theories — the production of physical ETC gauge bosons. Extended Technicolor is important because, in weak-interaction models where $SU(2) \times U(1)$ is broken dynamically, it offers the most straightforward method for communicating the symmetry breaking to ordinary matter.[1] The ETC bosons connect ordinary fermions to those which form the dynamic condensate.[2,3] Such a connection is necessary for models of Technicolor, where the dynamical symmetry breaking arises in the same manner as chiral symmetry breaking in QCD. It may be equally important if the symmetry breaking is of a more general character — for example, in a composite model of quarks and leptons.[1]

There are two extremes for models of the Technicolor interaction which produces the symmetry-breaking condensate. First, there are those with many doublets of technifermions: for example, an entire techni-family with the same $SU(3) \times SU(2) \times U(1)$ quantum numbers as the standard families. In this case, the signature of Technicolor is the spectrum and phenomenology of the pseudo-Goldstone bosons associated with the techni-family.[4,5] An ETC boson could be produced, along with a techniquark, in top-quark gluon collisions. However, these models have a serious weakness: they predict a charged scalar boson with mass between 5 and 14 GeV[6] which seems to be excluded by experiment.[7]

Alternatively, one may construct models with only a single techni-doublet. Such models have none of the above pseudo-Goldstone bosons and, in fact, no unusual particle content below ~1 TeV where one finds the Technicolor hadrons. (One may also avoid, though perhaps inelegantly, a problem often considered fatal to all Technicolor models: flavor-changing neutral currents.[8,9]) At the 1 TeV

scale, however, these models should show a rich structure. In particular, ETC gauge bosons which connect the ordinary colored quarks to the single, uncolored techni-doublet must themselves carry color. Such bosons could, in principle, be produced in hadronic collisions.

The purpose of this paper is to assess the cross-sections and backgrounds for producing these ETC bosons at SSC energies and to explain how such particles might be observed. In simple ETC models, the lightest ETC boson is the one that gives mass to the top quark; it may be as light as 1 TeV.[10] This boson is a prime target for SSC experiments.

We find that the cross-section for ETC boson pair production via two gluons is large. But careful consideration of this process yields additional assistance in finding signatures: ETC bosons are, as we shall show, produced dominantly as bound states with discrete masses. One of the ETCs may then decay by top-quark emission, leaving a bound-state of an ETC and a techniquark. The other ETC then decays, producing an anti-top and one or more Z^0s or W^+W^- pairs. The visibility of the signature is enhanced on two counts: (1) top quarks are produced at large transverse momentum, and (2) the invariant mass of the combination of top-quark jets and weak bosons will be that of the bound-state.

The plan of this paper is as follows: In section 2, we introduce some notation. In section 3, we isolate the dominant mechanism for producing ETC bosons and show that the resulting pair of ETC bosons forms a bound state. The cross-section for producing this bound-state resonance is given, in section 4, in terms of its wave-function in the non-relativistic approximation. In section 5, we examine the wave functions and spectroscopy of the $E\bar{E}$ and $E\bar{U}$ bound states using a version of the Richardson potential scaled to Technicolor. In section 6, we analyze

the branching ratios for different decay modes of the $E\bar{E}$ and $E\bar{U}$. At this point, we can calculate numerical estimates of the production cross-sections. Finally, in section 7, we examine backgrounds for these processes and show that they will not overwhelm the signature.

2. Notation

When we can, we will give results for a general ETC group. When we need a specific example, we will take the ETC group to be $SU(N+3)$ breaking to an $SU(N)$ of techni-color and an $SU(3)$ of color. (For numerical results and plots, we choose $N = 4$.) In this model, the ETC bosons E ($\bar{E}$) transform as a $\bar{3}$ (3) of color and an N ($\bar{N}$) of Technicolor. The techniquarks are neutral under color $SU(3)$ and form an $SU(2)_L$(weak) doublet

$$Q = \begin{pmatrix} U \\ D \end{pmatrix}$$

which transforms as an N under $SU(N)$. We assume that $SU(2)_L$ commutes with ETC.

For the general case, we introduce some notation for the group factors. Suppose one has a gauge group G which breaks to $\bar{G} \times \ldots$, where $\bar{G}$ is the gauge group of the gluons (eventually $SU(3)$). Suppose we wish to produce E bosons which are in an irreducible representation $\Re$ of $\bar{G}$. Then the cross-section depends on the invariants

$$\Delta_1 = \frac{C_2(\bar{G})C_2(\Re)}{n_{\bar{G}}} \qquad \Delta_2 = \frac{[C_2(\bar{G})]^2}{d_{\Re}} \tag{2.1}$$

where

$n_{\bar{G}}$ is the number of generators in $\bar{G}$

$d_{\Re}$ is the dimension of the representation $\Re$

and $C_2(\bar{G})$ and $C_2(\Re)$ are given by

$$C_2(\bar{G})\delta^{\bar{a}\bar{d}} = f^{\bar{a}\bar{b}\bar{c}} f^{\bar{d}\bar{b}\bar{c}} \qquad C_2(\Re)\delta^{\bar{a}\bar{d}} = f^{\bar{a}\hat{b}\hat{c}} f^{\bar{d}\hat{b}\hat{c}}. \tag{2.2}$$

Here, $\bar{a}$,$\bar{b}$,$\bar{c}$,$\bar{d}$ run over the generators of $\bar{G}$ and $\hat{b}$,$\hat{c}$ run over generators of G associated with the ETC bosons. For the case of $SU(N+3) \to SU(N)_{TC} \times SU(3)_C$, these group factors are

$$\Delta_1 = \frac{3N}{8} \qquad \Delta_2 = \frac{N}{6}. \tag{2.3}$$

3. Production mechanism

We imagine producing E bosons in pp collisions at CM energies between 10 and 40 TeV. In simple ETC models, the E boson which couples to a fermion f has a mass of order[2]

$$m_E^2 \sim \frac{\Lambda_{TC}^3}{m_f} \tag{3.1}$$

where $\Lambda_{TC} \sim 350$ GeV. It is then reasonable that the lightest E is the one which gives mass to the top quark and that its mass is of order 1 TeV. (Under our assumptions, this ETC boson must also couple to the left-handed b quark.[11] For now, we will concentrate only on the coupling to t quarks; the results for b quarks should be similar.)

Because of the large gluon content of the incident protons at high energies,[12] we consider first gluon-gluon collisions. Calculating the constituent amplitude for free $E\bar{E}$ production from the graphs of Figure 1 gives

$$\hat{\mathcal{M}}_{gg\to E\bar{E}} = g^4\left\{\Delta_1\left[-\frac{48}{1-x^2}\left(\frac{m^2}{\hat{s}}\right)^2 + 12\frac{m^2}{\hat{s}} - \frac{1}{2}\frac{3x^4+10x^2+19}{(1-x^2)}\right]\right.$$
$$\left.+\Delta_2\left[\frac{192}{(1-x^2)^2}\left(\frac{m^2}{\hat{s}}\right)^2 - \frac{48}{1-x^2}\frac{m^2}{\hat{s}} + 2\frac{3x^4+10x^2+19}{(1-x^2)^2}\right]\right\} \tag{3.2}$$

where m is the E boson mass, $x \equiv (t-u)/\hat{s}$, and $\sqrt{\hat{s}}$ is the gg subsystem CM energy.[13]

Gluon-gluon collision could also produce single E bosons (Figure 2). The dominant contribution to graphs 2a and 2b occurs when one of the incident gluons dissociates into a $t\bar{t}$ pair which are nearly colinear with it. In this case the constituent process is really $\bar{t}g \to E\bar{U}$ (Figure 3). Such processes are suppressed over those for $gg \to E\bar{E}$ by the ratio of top to gluon content in the incident protons. This suppression is roughly a factor of 100.[12]

The other $gg \to t\bar{U}E$ process (Figure 2c) is smaller than $gg \to E\bar{E}$ because of three effects: (1) it has an extra power of α_s over $gg \to E\bar{E}$, (2) because it has 3-body rather than 2-body phase space, the cross-section rises more slowly in the threshold region, and (3) 3-body phase space is intrinsically smaller by extra numerical factors.

The subprocess $t\bar{t} \to E\bar{E}$ is insignificant because of the small t quark content in the incident protons. The contribution of $q\bar{q} \to E\bar{E}$ for $q = u, d, etc.$ is also small because (1) the quark-quark luminosity is smaller than the gluon-gluon luminosity, and (2) the amplitude in leading order disappears at the $E\bar{E}$ production threshold.

In summary, we expect the largest production rate in the $gg \to E\bar{E}$ subprocess.

The cross-section for $pp \to E\bar{E}$ is obtained by convoluting the constituent cross-section with the gluon-gluon luminosity in pp collisions. In Figure 4, we plot $d\sigma/d\sqrt{\hat{s}}$ for the production of free ETCs via $gg \to E\bar{E}$, where $d\sigma$ is the differential pp cross-section including the effects of the parton distribution. (We also show $\bar{t}g \to E\bar{U}$ plus $tg \to \bar{E}U$ for comparison.) But it is clear from this plot that the ETCs should not be treated as free particles. The gluon-gluon luminosity at fixed $\sqrt{s}$ falls very rapidly with increasing $\sqrt{\hat{s}}$, so most of the production will occur for $\sqrt{\hat{s}}$ just above threshold. Thus, the E energies will be of order Λ_{TC}, the Technicolor scale. Their strong Technicolor interactions cannot then be ignored as long as the E bosons are sufficiently long-lived. We can estimate the lifetime from the decay rate of a free E:

$$\Gamma_{E\to\bar{t}U} = \frac{\alpha_s}{6} m_E \left(1 - \frac{m_U^2}{m_E^2}\right)^2 \left(1 + \frac{m_U^2}{2m_E^2}\right) \sim .01 m_E, \tag{3.3}$$

which is indeed small compared to $\Lambda_{TC} \sim 350$ GeV. So, at SSC energies, one properly should consider the physical states to be Technicolor singlet bound states of E boson pairs (or E bosons and techniquarks).

We conclude that the signal for ETC models with colored ETC bosons at a pp collider should be the production and decay of Technicolor singlet bound states.

4. Cross-sections for $gg \to E\bar{E}$ resonances

To calculate the cross-section for producing $E\bar{E}$ resonances, we use the Breit-Wigner formalism, for which we need to know the width of the decay of $E\bar{E}$ into two gluons. Let us approximate the $E\bar{E}$ bound states as nonrelativistic bound states with wave-function $\psi(r)$.[14] Then we can evaluate the width as

$$\Gamma_{E\bar{E}\to gg} = \frac{\pi\alpha_s^2|\psi(0)|^2}{2m_E^2}\delta_{group}\eta_{spin} \tag{4.1}$$

where

$$\delta_{group} = \begin{cases} 4n_{\bar{G}}\Delta_2, & \text{color singlet} \\ 4(n_{\bar{G}}-1)\Delta_2 - n_{\bar{G}}\Delta_1, & \text{color octet} \end{cases} \qquad \eta_{spin} = \begin{cases} 3, & \text{spin 0} \\ \frac{16}{5}, & \text{spin 2} \end{cases}.$$

For $SU(N+3) \to SU(N)_{TC} \times SU(3)_C$, the group parameters are

$$\delta_{group} = \begin{cases} \frac{16}{3}N, & \text{color singlet} \\ \frac{5}{3}N, & \text{color octet} \end{cases}.$$

Note that the spin 1 $E\bar{E}$ state is not produced in the leading order of perturbation theory.

The total cross-section for producing the $E\bar{E}$ resonance from pp collisions is given by a Breit-Wigner curve convoluted with the gluon-gluon luminosity[12]

$$\sigma_{pp\to tE\bar{U}} = \int_{m_{E\bar{E}}^2/s}^{1} \frac{d\mathcal{L}(\tau)}{d\tau}\,\hat{\sigma}(\tau s)\,d\tau \tag{4.2}$$

where $\tau = \hat{s}/s$ and $\sqrt{\hat{s}}$ is the subprocess CM energy. Near an $E\bar{E}$ resonance, the

subprocess cross-section is approximately

$$\hat{\sigma}(\hat{s}) = 2\frac{D_{E\bar{E}}}{256}\left(\frac{4\pi}{m^2_{E\bar{E}}}\right)\frac{\Gamma_{E\bar{E}\to gg}\Gamma_{E\bar{E}(tot)}}{(\sqrt{\hat{s}} - m_{E\bar{E}})^2 + \Gamma^2_{E\bar{E}(tot)}/4} \tag{4.3}$$

where $D_{E\bar{E}}$ is the spin and color degeneracy of the $E\bar{E}$ state being produced. In the limit of narrow width, the cross-section becomes

$$\sigma(s) = 32\pi^2\frac{D_{E\bar{E}}}{256}\left(\frac{\tau}{\hat{s}}\frac{d\mathcal{L}}{d\tau}\right)_{\hat{s}=m_{E\bar{E}}}\frac{\Gamma_{E\bar{E}\to gg}}{m_{E\bar{E}}} \tag{4.4}$$

5. $E\bar{E}$ and $E\bar{U}$ spectroscopy.

In order to estimate the splitting between the $1S$ and $2S$ $E\bar{E}$ states, we treat them as nonrelativistic bound states in a scaled-up version of the Richardson potential.[15] This potential and others[16] predict accurately the spectra of the $c\bar{c}$ and $b\bar{b}$ systems. If we assume that m_E is in the TeV range, the scaled-up versions should yield a rough guide to the $E\bar{E}$ spectrum. For the ψ and Υ systems, the Richardson potential is

$$V(q^2) = -\frac{4}{3}\left(\frac{12\pi}{33 - 2n_q}\right)\frac{1}{q^2}\frac{1}{\ln(1 + q^2/\Lambda^2_r)} \tag{5.1}$$

where $n_q = 3$ is the number of light quark flavors and $\Lambda_r = 398$ MeV fits the observed spectroscopy. For $SU(N+3) \to SU(N)_{TC} \times SU(3)_C$, this translates into a Technicolor binding force

$$V(q^2) = -\frac{N^2 - 1}{2N}\left(\frac{12\pi}{11N - 2n_Q}\right)\frac{1}{q^2}\frac{1}{\ln(1 + q^2/\Lambda^2_{r,TC})} \tag{5.2}$$

where $n_Q = 2$ is the number of light techniquarks and $\Lambda_{r,TC}$ is scaled up from Λ_r by the mass ratio ρ_T/ρ. Using large N arguments,[4,17] the ρ_T mass can be

estimated as

$$\frac{\rho_T}{\rho} \sim \frac{F_\pi}{f_\pi}\left(\frac{3}{N}\right)^{1/2} \tag{5.3}$$

where $f_\pi = 93$ MeV and $F_\pi \sim 247$ GeV. For $N = 4$, this gives $\rho_T \sim 1.77$ TeV and $\Lambda_{r,TC} \sim 915$ GeV. We then solve the Schrödinger equation with this potential and a nonrelativistic kinetic energy term. The $2S - 1S$ splitting is about 1.6 TeV for $m_E = 1$ TeV. Because of this large splitting and the rapidly falling gluon-gluon luminosity, the cross-section for producing a $2S$ $E\bar{E}$ is much smaller than for a $1S$.

The Technicolor hyperfine splitting may be treated as a perturbation and is calculated by analogy to meson mass differences arising from hyperfine splitting.[18] For Technicolor singlet states $Q\bar{Q}$ or $E\bar{U}$, the Technicolor hyperfine splitting term is

$$H_{HFS} = \alpha_N \left(\frac{N^2-1}{2N}\right)\frac{8\pi}{3}\delta^3(\vec{r})\frac{\vec{S}_1 \cdot \vec{S}_2}{m_1 m_2} \tag{5.4}$$

where the Technicolor group has been taken as $SU(N)$ and α_N is an effective coupling constant. For the $E\bar{E}$ state, the splitting is different due to the 4-boson contact term;[19] the complete expression is:

$$H_{HFS} = \alpha_N \left(\frac{N^2-1}{2N}\right)\frac{5\pi}{3}\delta^3(\vec{r})\frac{\vec{S}_1 \cdot \vec{S}_2}{m_1 m_2} \tag{5.5}$$

We estimate m_U and $\alpha_N|\psi(0)|^2$ from the $\rho_T - \pi_T$ splitting:

$$m = 2m_U + \frac{8\pi}{3}\left(\frac{N^2-1}{2N}\right)\alpha_N|\psi(0)|^2\frac{\vec{S}_1 \cdot \vec{S}_2}{m_U^2} \tag{5.6}$$

where $\vec{S}_1 \cdot \vec{S}_2$ is $-\frac{3}{4}$ for $\pi_T(Z^0)$ and $\frac{1}{4}$ for ρ_T. Using $N = 4$ and $\rho_T = 1.77$ TeV, this yields $m_U = 675$ GeV and $\alpha_N|\psi(0)|^2 = 0.049$ TeV^3. We assume analogous

formulas for $E\bar{E}$ and $E\bar{U}$ states but note that α_N and $|\psi(0)|^2$ will vary with the masses of the constituents. We could estimate the variation of $|\psi(0)|^2 \sim \mu^{1.5}$ from a potential model, but we do not know how to calculate the expected decrease of α_N with increasing μ (μ is reduced mass). Therefore we approximate $\alpha_N|\psi(0)|^2$ as a constant in calculating the $E\bar{E}$ and $E\bar{U}$ splittings.

In addition to the Technicolor interaction, the color force can split the color octet $E\bar{E}$ from the color singlet. This is like the $\pi^+ - \pi^o$ splitting. This term is

$$H_{color} = \left\{ \begin{array}{ll} +\frac{1}{6} & \text{(octet)} \\ -\frac{4}{3} & \text{(singlet)} \end{array} \right\} \alpha_s \left[\frac{1}{r} - \frac{5\pi}{3}\delta^3(\vec{r}) \frac{\vec{S}_1 \cdot \vec{S}_2}{m_1 m_2} \right]. \tag{5.7}$$

We use the wave-functions computed with the Richardson potential to estimate $\langle \frac{1}{r} \rangle$ and $|\psi(0)|^2$. In units of TeV, the results of solving the Schrödinger equation numerically can be closely parametrized as $\langle \frac{1}{r} \rangle \approx 1.21\mu^{0.44}$ and $|\psi(0)|^2 \approx 0.314\mu^{1.43}$ where μ is near 1 TeV. For $m_E = 1$ TeV, the color splitting is on the order of 100 GeV, several times smaller than the hyperfine splitting.

Assembling all of these contributions, we find $E\bar{E}$ and $E\bar{U}$ spectra, of which two examples are shown in Figure 5. Note that the S=0 color singlet state can be very much lighter than $2m_E$.

6. $E\bar{E}$ and $E\bar{U}$ decays.

The total width of the $E\bar{E}$ state includes the decays $E\bar{E} \to gg$, $E\bar{E} \to \bar{q}q$, $E\bar{E} \to Z^0Z^0$, and $E\bar{E} \to tE\bar{U}$ (Figure 6). The first two are unobservable in practice because of the large two jet background. We will show that the third mode is small, but it may be observable.

The last mode usually leads to the decay chain (if the $\bar{E}$ decays first)

$$(E\bar{E}) \to t + (E\bar{U}) \to t\bar{t} + \text{technipions.}$$

The technipions will appear as the longitudinal components of electroweak gauge bosons. The backgrounds for this mode should be small enough to make it a useful signature of the model (see below). In order to obtain a crude estimate of the partial width, we have again approximated the $E\bar{E}$ and $E\bar{U}$ systems as nonrelativistic bound states in a scaled up Richardson potential. In the dipole approximation ($E_t \sim m_{E\bar{E}} - m_{E\bar{U}} < \langle \frac{1}{r} \rangle$), we find

$$\Gamma_{E\bar{E}\to tE\bar{U}\text{ or }\bar{t}\bar{E}U} = 2\alpha_s \frac{(m_{E\bar{E}} - m_{E\bar{U}})^2}{m_U} \times |\langle \psi_{E\bar{E}} | \psi_{E\bar{U}} \rangle|^2 \times \begin{cases} 1, & J = 0 \to J = \frac{1}{2} \\ \frac{1}{3}, & J = 1 \to J = \frac{3}{2} \\ \frac{2}{3}, & J = 1 \to J = \frac{1}{2} \\ 1, & J = 2 \to J = \frac{3}{2} \end{cases} . \tag{6.1}$$

Since our approximations have been very crude, this result is only a rough guide. Using the potential model, we find the wave-function overlap $|\langle \psi_{E\bar{E}} | \psi_{E\bar{U}} \rangle|^2$ is typically greater than 0.9. For $m_E = 1$ TeV, Equation (6.1) gives widths on the order of 50 GeV. We neglect higher order processes where additional technipions ($W^{\pm}$,Z^0) are emitted. Besides a factor α_w, they are small because of the phase space factor.

To estimate the branching ratio for the $tE\bar{U}$ mode, we must estimate the widths of the other modes as well. $E\bar{E} \to gg$ has already been addressed in eqn. (4.1). It is about 100 GeV (singlet) or 30 GeV (octet) if $m_E = 1$ TeV. For $E\bar{E} \to \bar{q}q$, the graph of Figure 6b vanishes in the limit of zero internal $\vec{p}_E$ and

is therefore suppressed. For $E\bar{E} \to \bar{t}t$ through Figure 6d, we calculate for either color singlet or octet

$$\Gamma_{E\bar{E}\to t\bar{t}} = N\pi\alpha_s^2 \frac{|\psi(0)|^2}{m_E^2} \begin{cases} 3\frac{m_U^2}{m_E^2}, & \text{spin } 0 \\ \frac{4}{5}, & \text{spin } 2 \end{cases}. \tag{6.2}$$

Finally, there is $E\bar{E} \to Z^0Z^0$ or W^+W^-. We will crudely estimate this contribution by calculating $E\bar{E} \to \bar{U}U$ for free techni-quarks and then take $m_U \sim \frac{1}{2}m_{Z^0} \sim 0$ to reproduce the phase space of the Z's or W's. This gives for a color singlet $E\bar{E}$[20]

$$\Gamma_{E\bar{E}\to Z^0Z^0 \text{ or } W^+W^-} \sim 3\pi\alpha_s^2 \frac{|\psi(0)|^2}{m_E^2} \begin{cases} 0, & \text{spin } 0 \\ \frac{4}{5}, & \text{spin } 2 \end{cases}. \tag{6.3}$$

The color octet $E\bar{E}$ cannot decay in this mode. Both of the widths (6.2) and (6.3) are smaller than the decay into gg. The sum of the two is about 20 GeV if $m_E = 1$ TeV.

The total width of the $E\bar{E}$ state is enough smaller than the binding energy (which is the Technicolor scale) that the bound state treatment is indeed appropriate. (At $m_E = 1$ TeV, the total widths are 100-150 GeV.)

The $E\bar{U}$ bound state can decay into $\bar{t}$ + technipions or into $\bar{t}g$. We estimate the decay of the $J = \frac{1}{2}$ state into technipions using the method of effective low-energy lagrangians,[21] treating the $E\bar{U}$ as a nonrelativistic bound state. The technipions appear as the longitudinal components of the weak vector bosons. The result is

$$\begin{aligned} \Gamma_{E\bar{U}\to\bar{t}Z^0} &= \alpha_s \frac{m_E + m_U}{m_E} \left(\frac{3N}{64}\right) \frac{|\psi(0)|^2}{F_\pi^2}, \\ \Gamma_{E\bar{U}\to\bar{t}Z^0Z^0} &= \Gamma_{E\bar{U}\to\bar{t}Z^0} \left(\frac{m_E + m_U}{2F_\pi}\right)^2 \left(\frac{1}{48\pi^2}\right) \frac{1}{8}, \end{aligned} \tag{6.4}$$

where $F_\pi \sim 247$ GeV. Note that the factor $1/48\pi^2$ is due to the 3-body phase

space. Allowing more technipions in the final state only increases this numerical suppression, so we conclude that the $\bar{t}Z^0$ final state is the only significant one.

The $J = \frac{3}{2}$ decay into $\bar{t}$ + technipions is more difficult to estimate. Equation (3.3) gives a very rough estimate ignoring all the bound state effects. In any case, because the $J = \frac{3}{2}$ mass is significantly above the $J = \frac{1}{2}$ mass, the $E\bar{E}$ state will most often decay into the $J = \frac{1}{2}$ $E\bar{U}$ state (see Equation (6.1) and Figure 5). Therefore the $J = \frac{3}{2}$ width is not very interesting.

The $E\bar{U} \to \bar{t}g$ diagrams are the inverse of those shown in Figure 3. Again treating the $E\bar{U}$ as a nonrelativistic bound state, we find

$$\Gamma_{E\bar{U}\to\bar{t}g} = 4\pi\alpha_s^2 \frac{N}{2} \frac{|\psi(0)|^2(m_E + m_U)}{m_E^3} \begin{cases} \frac{m_U^2}{(m_E+m_U)^2}, & J = \frac{1}{2} \\ \frac{1}{3}, & J = \frac{3}{2} \end{cases}. \tag{6.5}$$

For $m_E = 1$ TeV, $\Gamma_{E\bar{U}\to\bar{t}g}/\Gamma_{E\bar{U}\to\bar{t}Z^0} \sim 1/6$.

We are now ready to compute the cross section times the branching ratio. $d\hat{\sigma}/d\sqrt{\hat{s}}$ for $gg \to t\bar{t}Z^0$ is shown in Figure 7. It turns out to be very large, about 4 nb for $m_E = 1$ TeV and $sqrts = 40$ TeV. Figure 8 shows the relative sizes of the resonances. For the larger values of m_E, the splittings become smaller and the relative sizes are mostly determined by the degeneracies. For $m_E \sim 1$ TeV, the hyperfine splitting is so big that the falling gg luminosity causes the $S = 0$ states to dominate the $S = 2$ states. In Figure 9 we see that at $\sqrt{s} = 20$ TeV the signal is above 1000 events until $m_E > 2.3$ TeV.

7. Backgrounds

The most promising signal is a set of resonances in the $t\bar{t}Z^0$ channel. There are several standard model processes with this same $t\bar{t}Z^0$ final state. Figure 10 shows examples of simple 2-jet $t\bar{t}$ production with the Z^0 attached to one of the fermions. These processes are smaller than $E\bar{E}$ production by a factor of α_w and by 3-body phase space factors. As an example, we have calculated the contribution from $gg \to t\bar{t}Z^0$ requiring $p_\perp > 50$ GeV for both top quarks. Figure 7 displays this cross-section alongside the signal for $\sqrt{s} = 10, 20$, and 40 TeV. These backgrounds are clearly not a problem. Alternatively, we can consider making a $t\bar{t}$ pair from one Z^0 in a standard Z^0Z^0 production diagram (Figure 11). However, even neglecting the branching fraction for $Z^0 \to t\bar{t}$, $d\hat{\sigma}/d\sqrt{\hat{s}}$ for Z^0Z^0 production is more than 3 orders of magnitude smaller than the signal shown in Figure 7.[12]

Note that very similar backgrounds present problems in the search for Higgs bosons at SSC.[22] However the Higgs boson production cross-section is only a few picobarns, whereas for $m_E = 1$ TeV and $\sqrt{s} = 40$ TeV the $E\bar{E}$ cross-section is larger than 1 nb.

There are also questions about distinguishing the $t\bar{t}Z^0$ final state from other processes. In order to avoid the multijet QCD background, the top quarks could be tagged in their semileptonic decay modes. It may in fact be possible to achieve a signal-to-noise enhancement of ~ 60 in distinguishing a pair of top quark jets from light quark jets.[23] The algorithm requires an isolated hard lepton from one top quark decay, so it picks up only $\sim 15\%$ of the signal. Because of this inefficiency, one might have to observe the Z^0 in its hadronic as well as its leptonic decays. Alternatively one could tag the e^+e^- or $\mu^+\mu^-$ modes of the Z^0 and allow hadronic t decays. Note that if the hadronic t decays are tagged by the

separated decay of the daughter b quark, b and t quark jets will look alike. Then backgrounds and signals with b quarks must be added to those with t quarks. In this regard we observe that the standard model $b\bar{b}Z^0$ background arises in the same way as the $t\bar{t}Z^0$ background considered above and will be the same size.

There is also a decay mode $E\bar{E} \rightarrow Z^0Z^0$ or W^+W^- for the color singlet $E\bar{E}$ states. The partial width is smaller than for the $t\bar{t}Z^0$ mode. To avoid the 4-jet QCD background, one Z^0 or $W^\pm$ would have to decay leptonically. This part of the cross section would then be on the order of 30 pb, which is still somewhat larger than the $gg \rightarrow llqq$ backgrounds which are a problem for Higgs detection.[22]

8. Conclusion

This work suggests that when experiments at SSC are testing the Technicolor hypothesis, they could at the same time look for the signatures of ETC models. $E\bar{E}$ production would be tagged by the $t\bar{t}Z^0$ final state and one may observe the spectroscopy and decay of the $E\bar{E}$ and $E\bar{U}$ bound states if invariant masses can be reconstructed.

As already pointed out, there are small quantitative modifications to our results depending on details (chirality and mixing) of the couplings of the ETC bosons to t and b quarks. One would expect additional decay modes with b quarks instead of t quarks, which may look very similar in practice to the t quark modes with hadronic t decays. In some of these modes $W^\pm$ would replace Z^0.

ACKNOWLEDGEMENTS

We would like to thank Michael Peskin and Savas Dimopoulos for many useful ideas and conversations.

REFERENCES

1. For mechanisms other than ETC, see the review in
   P. Sikivie, in *Proceedings of the 1984 Summer Study on the Design and Utilization of the Superconducting Super Collider, Snowmass, Colorado*, edited by R. Donaldson and J. Morfin (Fermilab, 1985), p. 771.
2. S. Dimopoulos and L. Susskind, *Nucl. Phys.* **B155** (1978) 237;
   E. Eichten and K. Lane, *Phys. Lett.* **90B** (1980) 125.
3. For reviews of Technicolor and ETC, see
   E. Farhi and L. Susskind, *Phys. Rep.* **74** (1981) 277;
   R. Kaul, *Rev. Mod. Phys.* **55** (1981) 158;
   K. Lane, in *Proceedings of the 1982 Summer Study Elementary Particle Physics and Future Facilities, Snowmass, Colorado*, edited by R. Donaldson, R. Gustafson and F. Paige (AIP, DPF, New York 1983), p. 222.
4. S. Dimopoulos, *Nucl. Phys.* **B168** (1980) 69.
5. M. Peskin, *Nucl. Phys.* **B175** (1980) 97;
   J. Preskill, *Nucl. Phys.* **B177** (1981) 21.
6. E. Eichten and K. Lane, *Phys. Lett.* **90B** (1980) 125;
   S. Chadha and M. Peskin, *Nucl. Phys.* **B187** (1981) 541;
   P. Binetruy, S. Chadha and P. Sikivie, *Phys. Lett.* **107B** (1981) 425.
7. S. Yamada, in *1983 International Symposium on Lepton and Photon Interactions at High Energies, Ithaca, New York*, edited by D. Cassel and D. Kreinick (Newman Lab Nucl. Studies, Cornell, 1983), p. 525;
   S. Komamiya, in *1985 International Symposium on Lepton and Photon Interactions at High Energies, Kyoto, Japan,* to be published.

8. S. Dimopoulos, H. Georgi and S. Raby, *Phys. Lett.* **B127** (1983) 101.

9. S. Chao and K. Lane,, *Phys. Lett.* **159B** (1985) 135;
   B. Holdom, *Phys. Rev.* **D24** (1981) 1441.

10. S. Dimopoulos and J. Ellis, *Nucl. Phys.* **B182** (1981) 505.

11. The model we consider here is oversimplified. We have assumed that ETC commutes with $SU(2)_L$. On the other hand, the t and b quarks should not couple to exactly the same ETCs; otherwise, they will have the same mass. A model which satisfies these constraints is given in [8]. Some ETCs couple equally to left-handed b's and t's, others couple only to right-handed t's, and yet others couple only to right-handed b's. Quark masses arise because these ETCs mix. Rather than make a detailed analysis of a particular model, we make the simplifying assumption that the ETCs couple vectorially, coupling to t's and possibly b's. Our conclusions do not depend on whether the couplings are vectorial or chiral.

12. E. Eichten, I. Hinchliffe, K. Lane and C. Quigg, *Rev. Mod. Phys.* **56** (1984) 579. For numerical calculations we use the parton distribution functions of Set 2 and $\alpha_s(q^2)$ given by their Eqn. (2.42).

13. The states are normalized so that $< p|q >= (2\pi)^3 2\omega\delta^3(p-q)$, and the amplitude has been averaged over gluon spin and color.

14. normalized to $\int d^3r|\psi(r)|^2 = 1$

15. J. L. Richardson, *Phys. Lett.* **82B** (1978) 272.

16. For a review of potential models, see
    E. Eichten in *Proceedings of the 1984 SLAC Summer Institute on Particle Physics, Stanford*, edited by P. McDonough (SLAC, Stanford, 1985), p. 1.

17. S. Dimopoulos, S. Raby, G. Kane, *Nucl. Phys.* **B182** (1981) 77.

18. A. De Rujula, H. Georgi and S. L. Glashow, *Phys. Rev.* **D12** (1975) 147.

19. There is also a contribution due to exchange of the effective Higgs boson which breaks ETC. This contribution turns out to be relatively small unless the mass of the Higgs boson is near the mass of the $E\bar{E}$ bound state (in which case mixing could occur between the Higgs and the $E\bar{E}$). We ignore this possible complication.

20. The zero width for the spin 0 state is an artifact of our method, in particular taking $m_U \sim 0$. Because the nonzero results we obtain for the other states are small, we will not be concerned with trying to improve the approximation.

21. See, for example,

    S. Coleman, J. Wess and B. Zumino, *Phys. Rev.* **177** (1969) 2239;

    C. Callan, S. Coleman, J. Wess and B. Zumino, *Phys. Rev.* **177** (1969) 2247.

22. J. F. Gunion, P. Kalyniak, M. Soldate, and P. Galison, SLAC-PUB-3604, March 1985;

    J. F. Gunion, Z. Kunszt, and M. Soldate, SLAC-PUB-3709, June 1985.

23. K. Lane and J. Rohlf, in *Proceedings of the 1984 Summer Study on the Design and Utilization of the Superconducting Super Collider, Snowmass, Colorado*, edited by R. Donaldson and J. Morfin (Fermilab, 1985), p. 737.

FIGURE CAPTIONS

1. Feynman diagrams for $gg \to E\bar{E}$
2. Feynman diagrams for $gg \to t\bar{U}E$
3. Feynman graphs for associated production $\bar{t}g \to \bar{U}E$.
4. $d\sigma/d\sqrt{\hat{s}}$ for free ETCs with $m_E = 1$ TeV, $\sqrt{s} = 40$ TeV and $N = 4$. For comparison, the dashed line shows $\bar{t}g \to E\bar{U}$ plus $tg \to \bar{E}U$.
5. $E\bar{E}$ and $E\bar{U}$ spectra for $m_E = 1$ TeV and 2 TeV with $N = 4$.
6. $E\bar{E}$ decay modes.
7. Cross-section for $pp \to E\bar{E} \to t\bar{t}Z^0$ (solid) compared to the gg part of standard model $pp \to t\bar{t}Z^0$ (dashed), taking $m_E = 1$ TeV. There is a $p_\perp > 50$ GeV cut for the top quarks in the $gg \to t\bar{t}Z^0$ calculation. The 3 curves are for $\sqrt{s} = 10, 20, 40$ TeV with $N = 4$. The resonances are (1) the $J = 0$ singlet, (2) the $J = 0$ octet, and (3) the $J = 1$ singlet and octet.
8. Number of $pp \to E\bar{E} \to t\bar{t}Z^0$ events under each resonance for $\sqrt{s} = 40$ TeV, $\int \mathcal{L}\, dt = 10^{40}\text{cm}^{-2}$ and $N = 4$, showing dependence on m_E.
9. Number of $pp \to E\bar{E} \to t\bar{t}Z^0$ events under all resonances for $\sqrt{s} = 10$, 20, and 40 TeV. $\int \mathcal{L}\, dt = 10^{40}\text{cm}^{-2}$ and $N = 4$.
10. Examples of $t\bar{t}Z^0$ production in the standard model.
11. Standard model $t\bar{t}Z^0$ production through an intermediate Z^0.

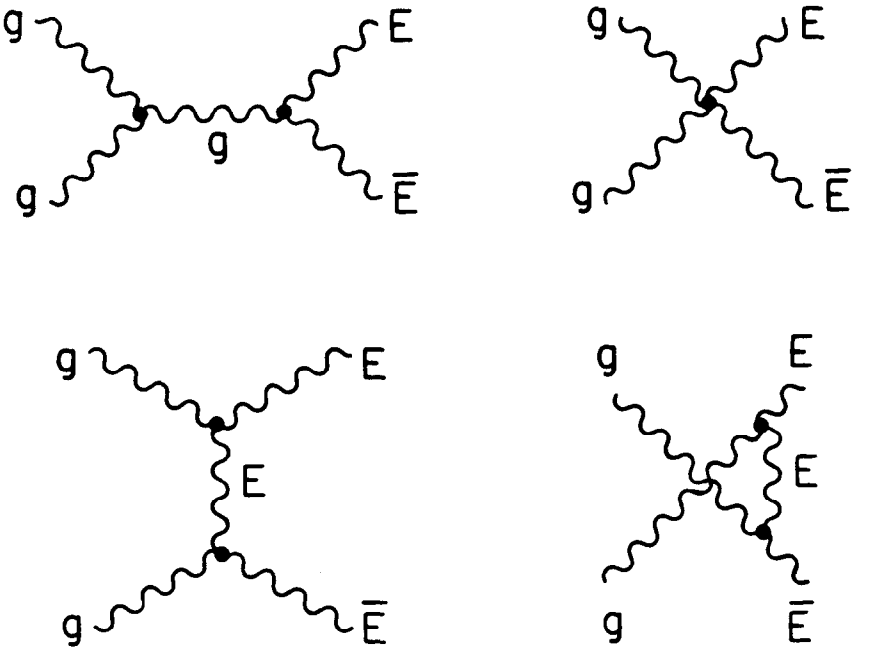

Figure 1.

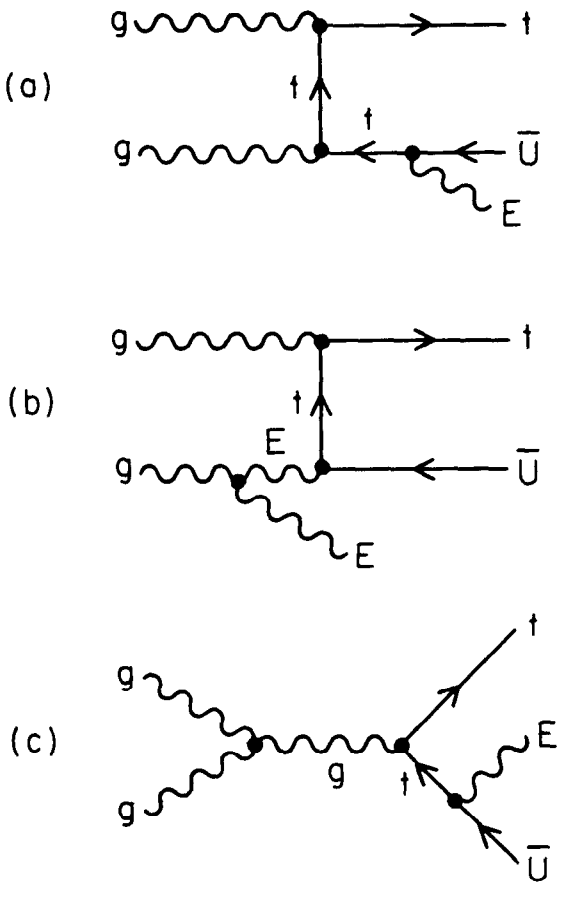

Figure 2.

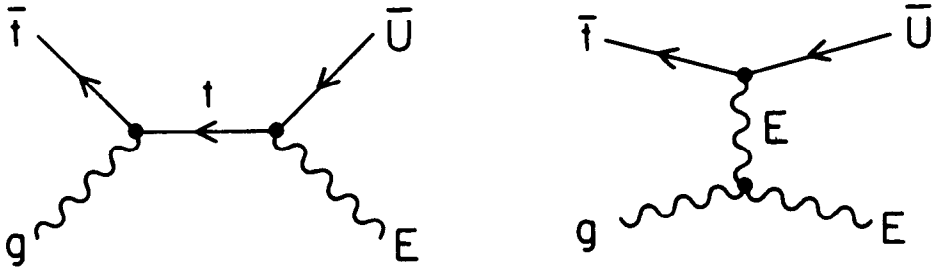

5283A3

11-85

Figure 3.

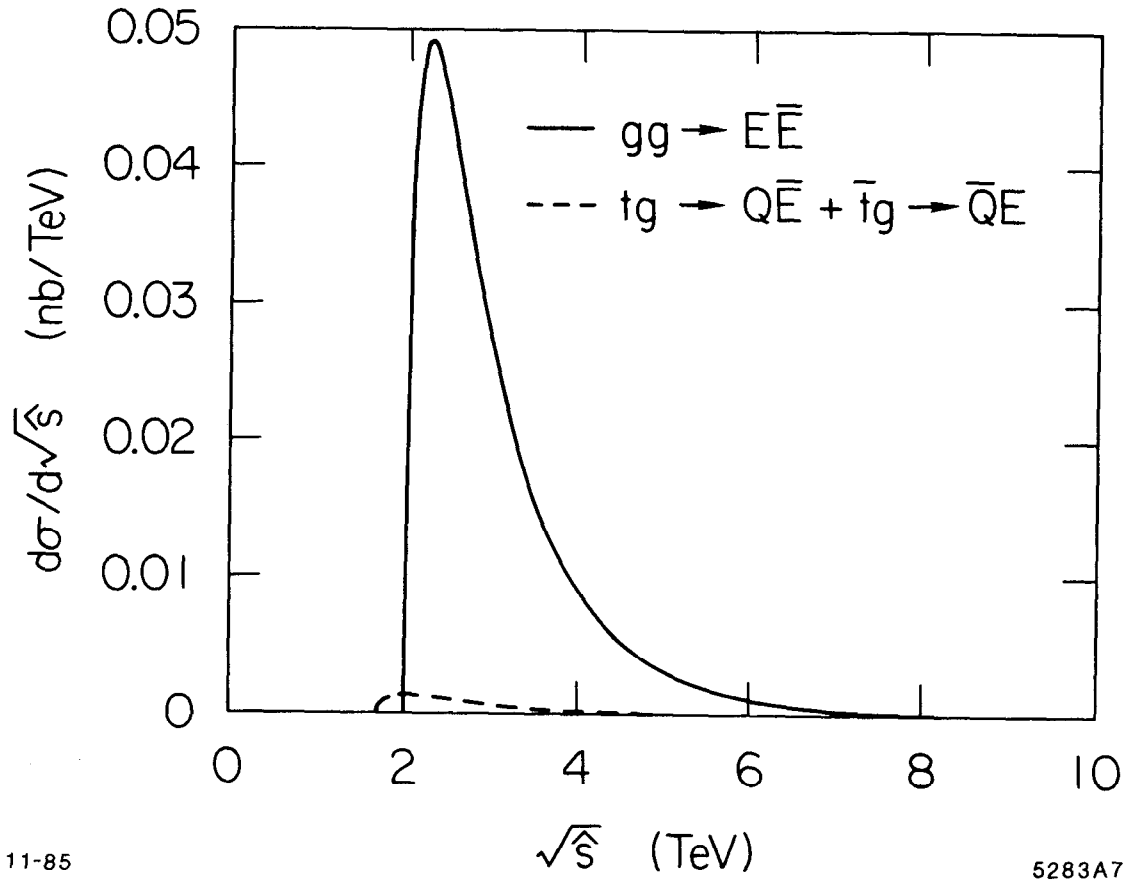
0.05
0.04
0.03
0.02
0.01
0
dσ/d√ŝ (nb/TeV)
gg → EĒ
tg → QĒ + t̄g → Q̄E
0
2
4
6
8
10
√ŝ (TeV)
11-85
5283A7

Figure 4.

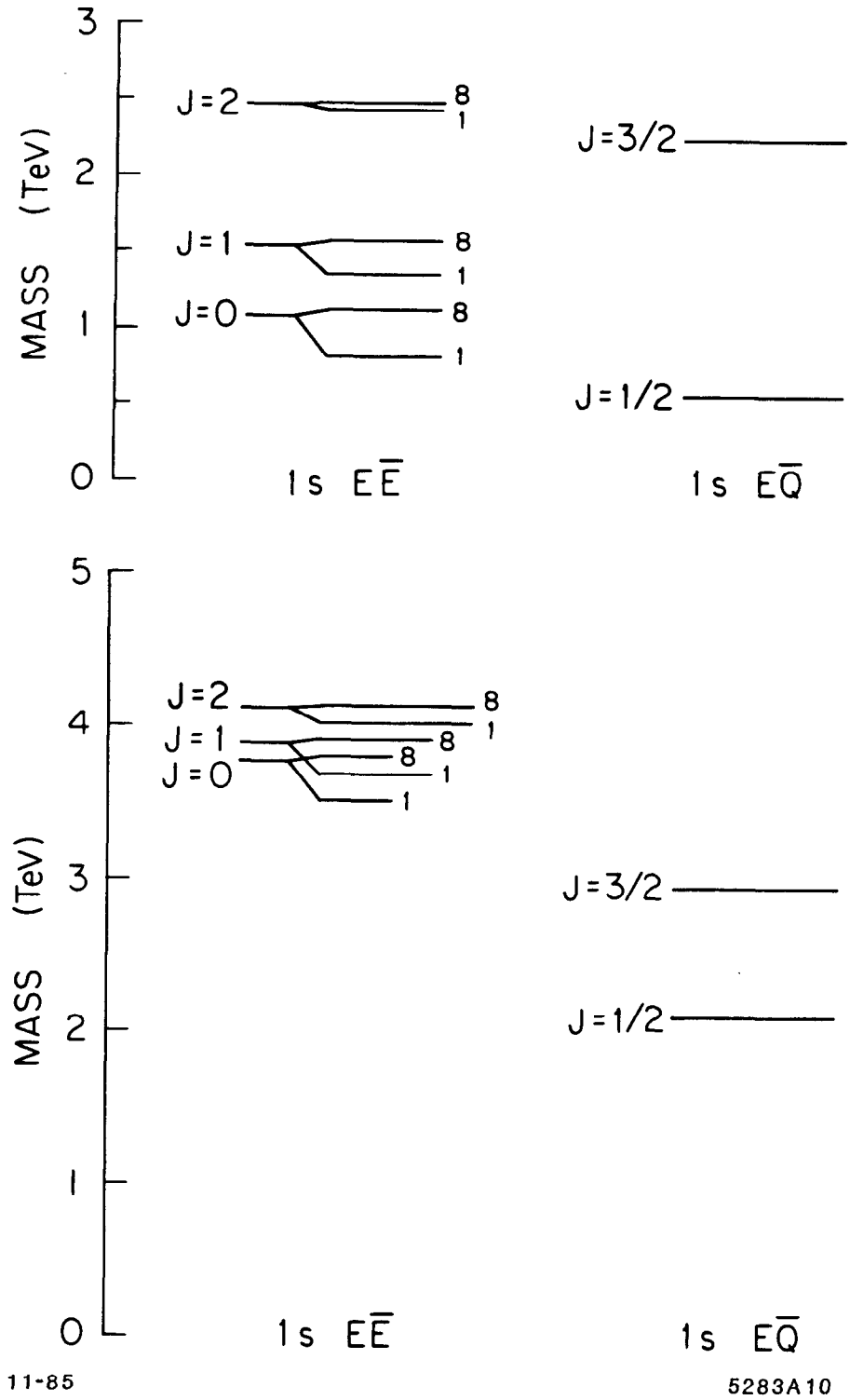
MASS (TeV)
3
2
1
0
J=2
8
1
J=1
8
1
J=0
8
1
1s EĒ
J=3/2
J=1/2
1s EQ̄
MASS (TeV)
5
4
3
2
1
0
J=2
8
1
J=1
8
8
1
J=0
1
1s EĒ
J=3/2
J=1/2
1s EQ̄
11-85
5283A10

Figure 5.

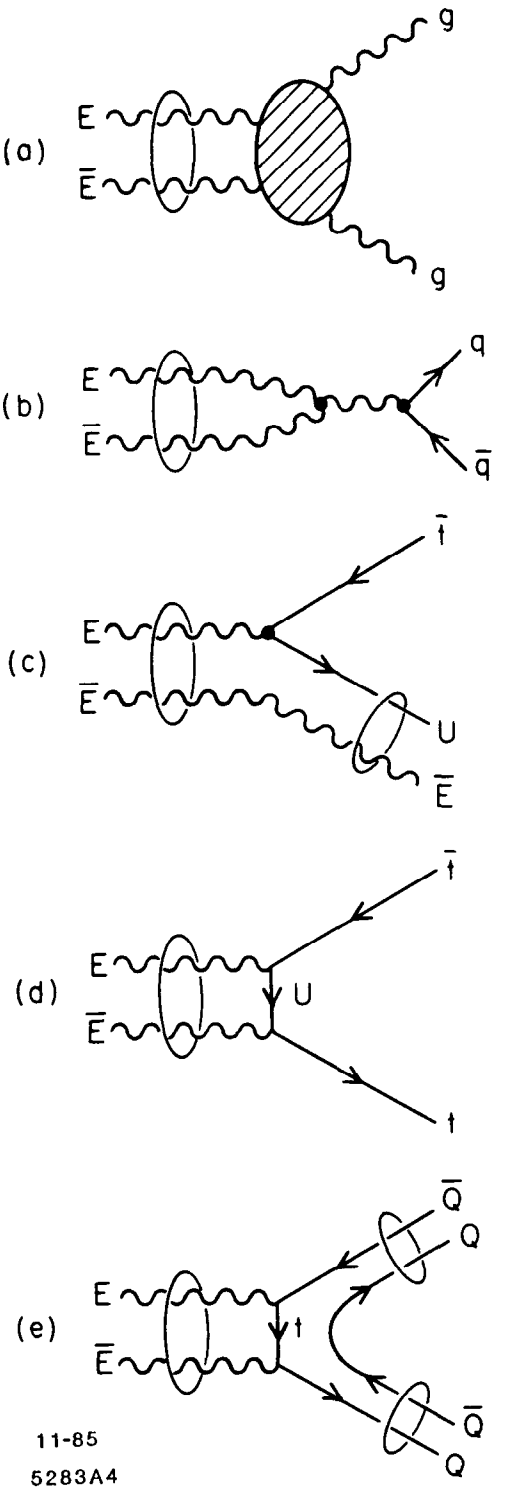
(a)
E
$\bar{E}$
g
g
(b)
E
$\bar{E}$
q
$\bar{q}$
(c)
E
$\bar{E}$
$\bar{t}$
U
$\bar{E}$
(d)
E
$\bar{E}$
U
$\bar{t}$
t
(e)
E
$\bar{E}$
t
$\bar{Q}$
Q
$\bar{Q}$
Q
11-85
5283A4

Figure 6.

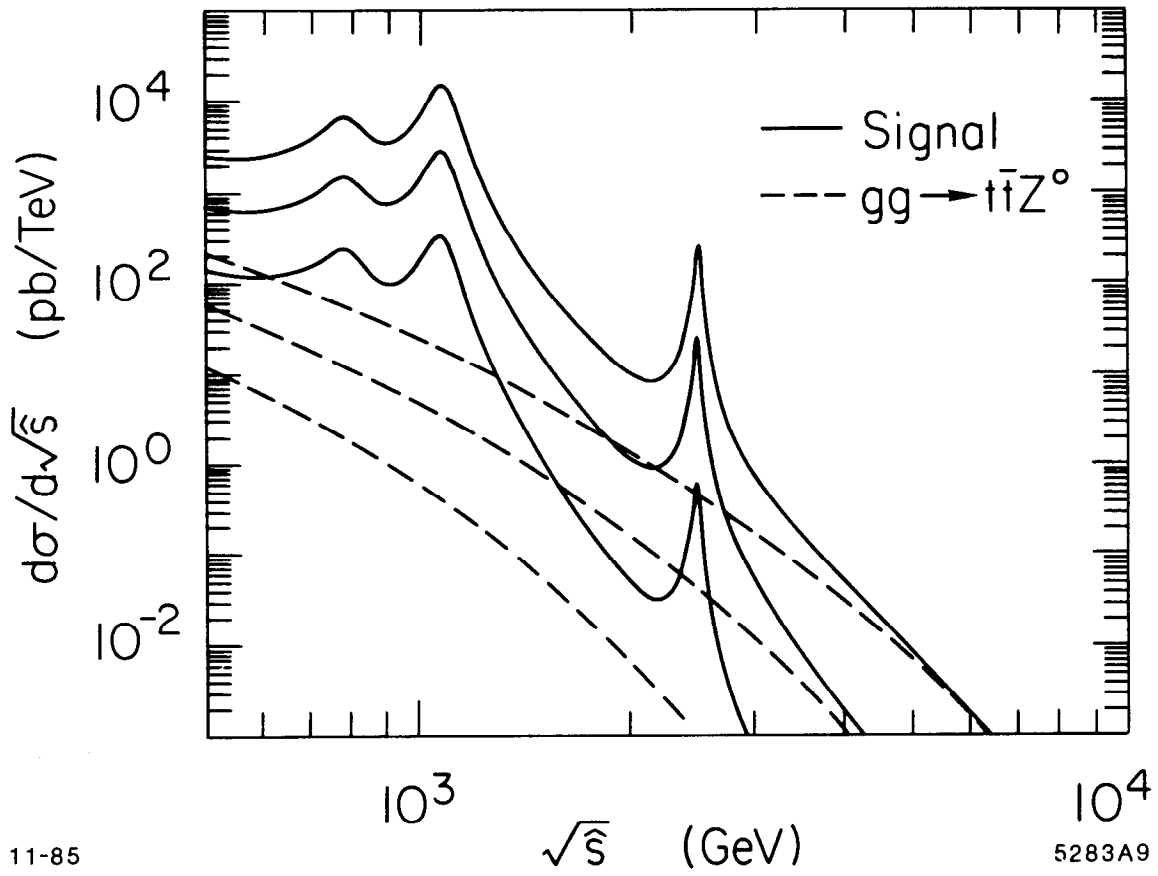
Signal
gg→tt̄Z°
10^4
10^2
10^0
10^{-2}
$d\sigma/d\sqrt{\hat{s}}$ (pb/TeV)
10^3
10^4
$\sqrt{\hat{s}}$ (GeV)
11-85
5283A9

Figure 7.

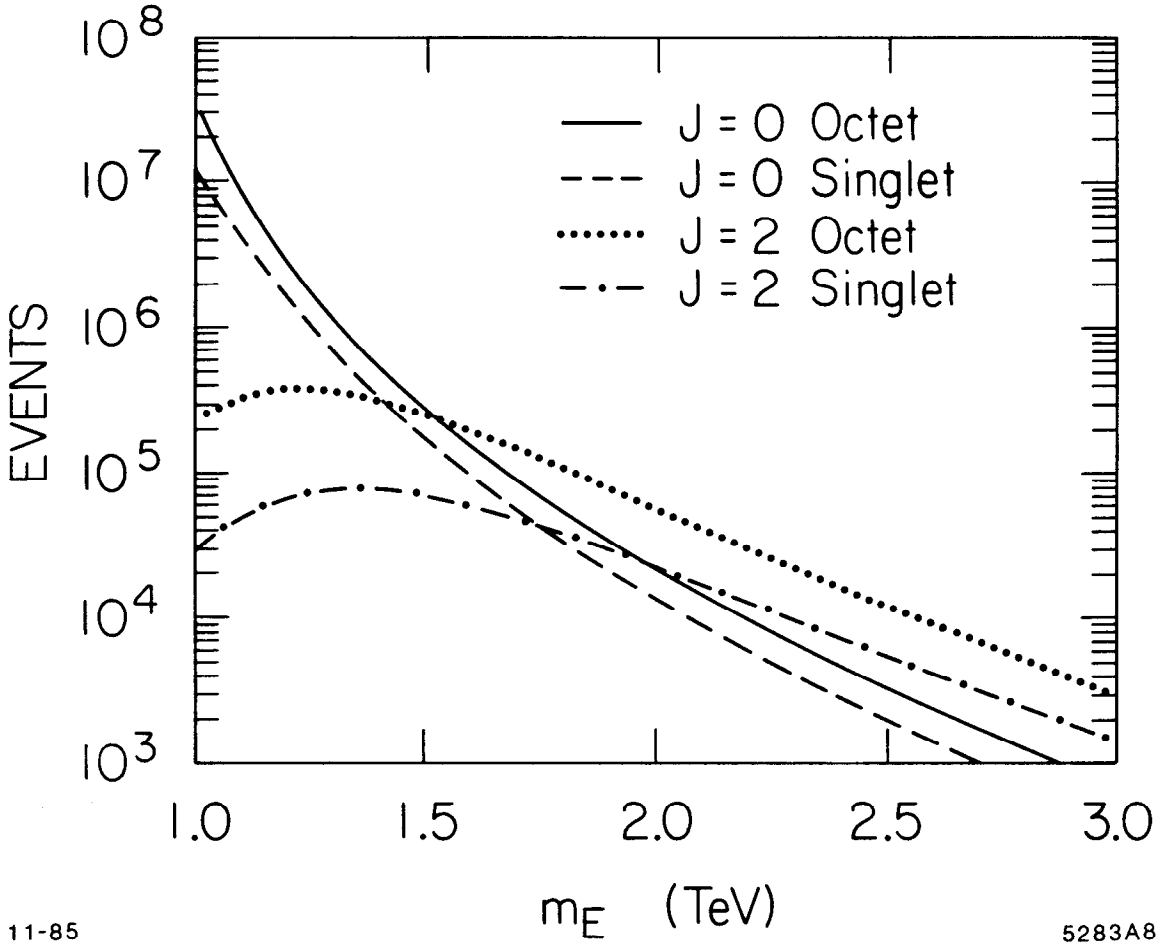
10^8
10^7
10^6
10^5
10^4
10^3
EVENTS
J = 0 Octet
J = 0 Singlet
J = 2 Octet
J = 2 Singlet
1.0
1.5
2.0
2.5
3.0
m_E (TeV)
11-85
5283A8

Figure 8.

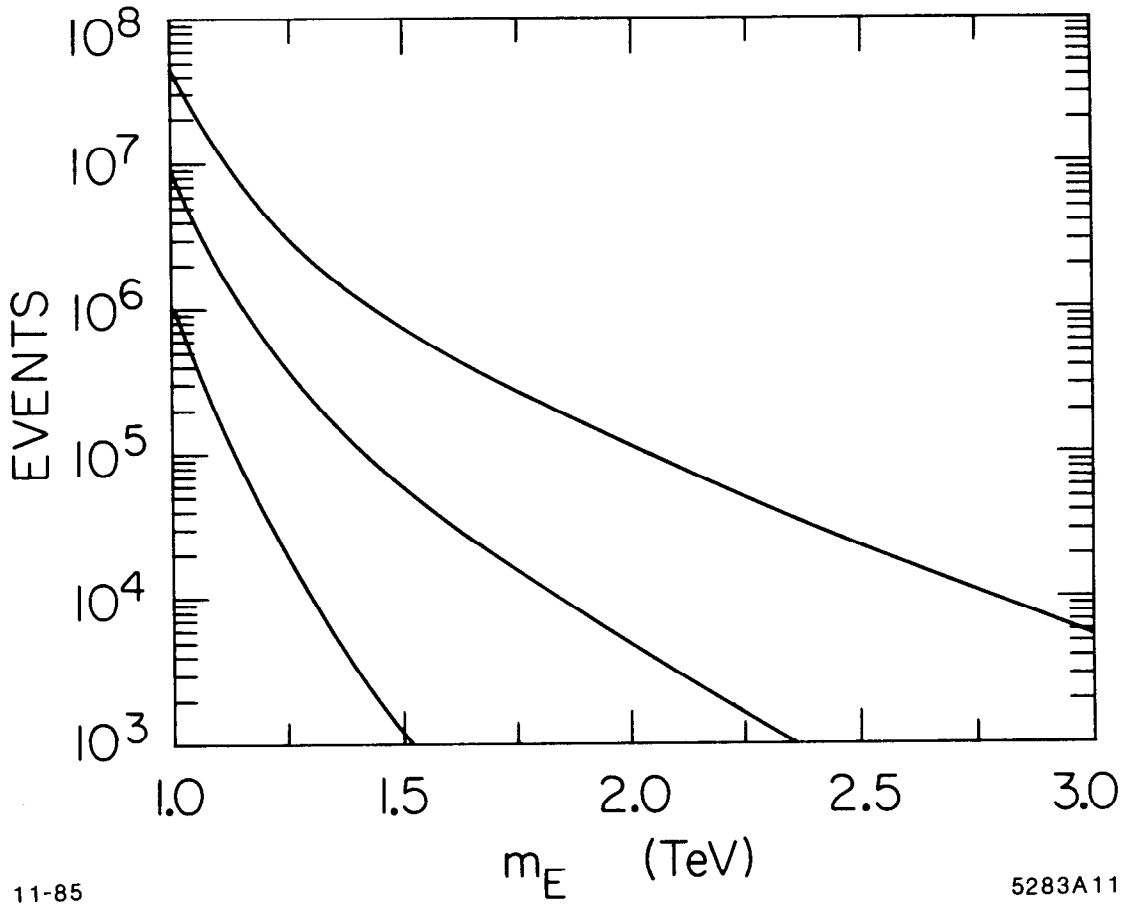
10^8
10^7
10^6
10^5
10^4
10^3
EVENTS
1.0
1.5
2.0
2.5
3.0
m_E (TeV)
11-85
5283A11

Figure 9.

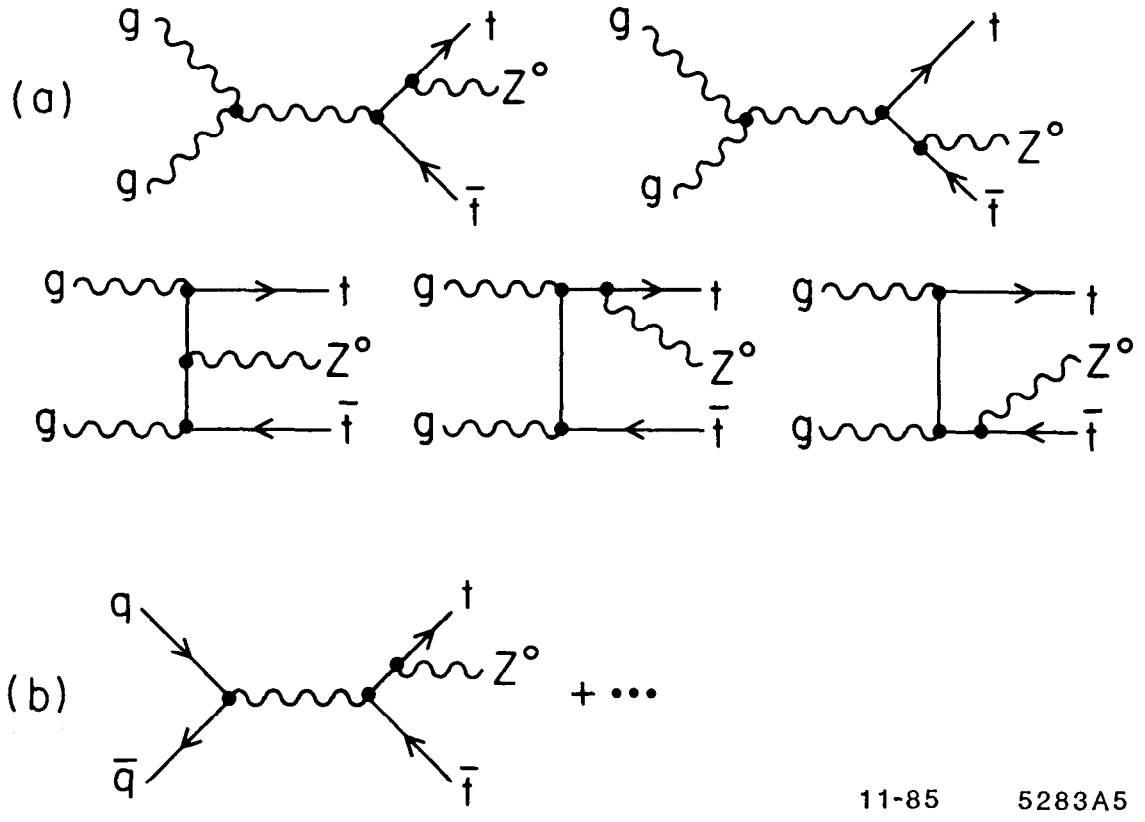

Figure 10.

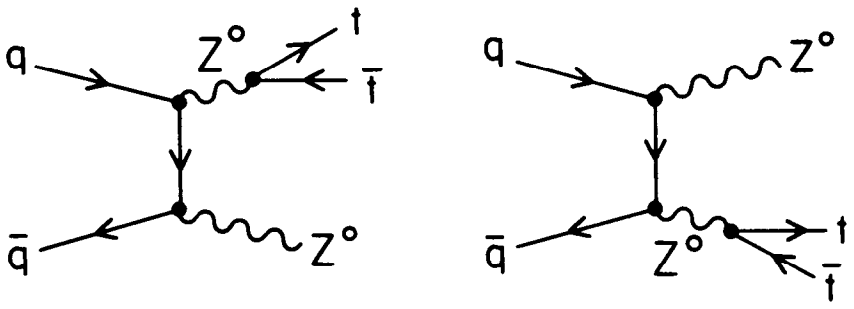

Figure 11.